A Control Allocation approach to induce the center of pressure position and shape the aircraft transient response

Varriale, Carmine; Voskuijl, Mark

DOI
10.1016/j.ast.2021.107092

Publication date
2021

Document Version
Final published version

Published in
Aerospace Science and Technology

Citation (APA)
Varriale, C., & Voskuijl, M. (2021). A Control Allocation approach to induce the center of pressure position and shape the aircraft transient response. *Aerospace Science and Technology*, *119*, Article 107092. https://doi.org/10.1016/j.ast.2021.107092

Important note
To cite this publication, please use the final published version (if applicable).
Please check the document version above.

Aerospace Science and Technology 119 (2021) 107092

Contents lists available at ScienceDirect

Aerospace Science and Technology

www.elsevier.com/locate/aescte

A Control Allocation approach to induce the center of pressure position and shape the aircraft transient response

Carmine Varriale [a,*], Mark Voskuijl [b]

[a] Faculty of Aerospace Engineering, Delft University of Technology, Delft, the Netherlands
[b] Faculty of Military Sciences, Netherlands Defence Academy, Den Helder, the Netherlands

ARTICLE INFO

Article history:
Received 17 December 2020
Received in revised form 14 July 2021
Accepted 31 August 2021
Available online 9 September 2021
Communicated by Christian Circi

Keywords:
Flight mechanics
Control Allocation
Direct Lift Control
Box-wing

ABSTRACT

This paper presents a Control Allocation formulation aimed at altering the dynamic transient response of an aircraft by exclusive means of the aerodynamic effectiveness of its control effectors. This is done, for a given Flight Control System architecture and, optionally, closed-loop performance, by exploiting the concept of Control Center of Pressure, i.e. the center of pressure due to only aerodynamic control forces. Two formulations are proposed, and their advantages and disadvantages presented. The first is based on the straightforward augmentation of the control effectiveness matrix, the second on a weighting matrix to prioritize control effectors. The latter is implemented in three application studies on a box-wing aircraft configuration with redundant control surfaces: a simple pull-up maneuver, a trajectory tracking task, and an altitude holding task in turbulent atmosphere. Results show that the proposed formulation can significantly impact performance metrics that are closely related to the aircraft transient response. In the best case scenario, the aircraft is able to completely cancel the non-minimum phase behavior typical of pitch dynamics, hence achieving a sharp initial response to longitudinal commands. If compared to a standard Control Allocation algorithm, the proposed formulation results in improved tracking precision, better disturbance rejection, and a measurably improved feeling of comfort on board.

1. Introduction

Disruptive aircraft configurations are becoming increasingly popular in modern research studies, from future commercial concepts to unmanned aircraft systems applications. This is due to the inherent performance benefits that they may allow to obtain, but also to their potential capability of reshaping the aeronautical sector in a more profound way. Examples are represented by the Blended Wing Body configuration [1], the more recent Flying-V concept [2], and a wide range of non-planar wing geometries. While the concepts proposed in this paper are applicable to any aircraft configuration, the present investigation focuses on a transonic commercial transport box-wing aircraft model, referred to as the PrandtlPlane (PrP) and shown in Fig. 1.

Brought to fame by an intuition of Ludwig Prandtl [3], the box-wing has been proven to generate the least induced drag for a given span and lift [4]. This property has constituted the scientific ground of several engineering research efforts, aimed at integrating its complex geometry in complete aircraft and compound rotorcraft architectures [5–7]. The unique aerodynamic properties of the box-wing allow the PrP to be competitive in the modern commercial aviation market [8]. Additionally, the possibility to install redundant control surfaces, inboard and outboard on both the front and rear wings, allows the PrP to make use of unconventional piloting techniques such as Direct Lift Control (DLC) [9,10].

DLC is defined as the capability to use control effectors to directly control the aircraft lift. This is a common technique for helicopter pilots, for example, who are able to control vertical dynamics directly through the collective command. Vertical control of conventional airplanes, instead, revolves around the use of a tail elevator to generate a small, dislocated control lift. While this lift contribution is generally small, it produces a significant pitch moment and gives raise to some angle of attack dynamics. This very indirect control technique results in the classic, undesired non-minimum phase behavior of pitch dynamics, with the initial aircraft response (due to control effectors dynamics) being opposite to the much larger steady-state response (due to angle of attack dynamics).

With respect to symmetric motion in the vertical plane, the most complete fundamental analysis about DLC shows that its performance mainly depends on the longitudinal position of the Control Center of Pressure (CCoP) [11]. This is the center of pressure of

* Corresponding author.
E-mail addresses: C.Varriale@tudelft.nl (C. Varriale), M.Voskuijl@mindef.nl (M. Voskuijl).

https://doi.org/10.1016/j.ast.2021.107092

Nomenclature

Symbols

a	generic acceleration	m/s^2
α	angle of attack	rad
b	reference wingspan	m
B	control effectiveness matrix	1/rad
β	angle of sideslip	rad
$\overline{c}$	mean aerodynamic chord	m
$C_{(\cdot)}$	generic non-dimensional coefficient	-
δ, $\boldsymbol{\delta}$	control effectors actual displacements	rad
g	gravitational acceleration	m/s^2
γ	flight path angle	rad
h	altitude	m
I	identity matrix	-
J_{yy}	moment of inertia about the y_B axis	kg m^2
K	controller gain	-
κ	matrix condition number	-
$\mathcal{L}, \mathcal{M}, \mathcal{N}$	roll, pitch, yaw moments	N m
$\boldsymbol{\mathcal{M}}$	generalized forces and moments	N or N m
m	mass	kg
M	Mach number	-
n	load factor	-
N	generic quantity	-
ν, $\boldsymbol{\nu}$	generic control allocation objectives	
p, q, r	roll, pitch, yaw rotational speeds	rad/s
q_∞	asymptotic dynamic pressure	N/m^2
S	reference surface area	m^2
t	time	s
θ	angle of elevation	rad
u, $\boldsymbol{u}$	control effectors ideal displacements	rad
V	airspeed	m/s
$W_{\boldsymbol{u}}$	weighting matrix	-
x_B, y_B, z_B	longitudinal, lateral, normal body axes	
Z	normal force in body axes	N

Subscripts and superscripts

cr	cruise
des	desired
MTO	maximum at take-off
pax	passengers
pk	peak
ref	reference
tr	trim

Abbreviations

AMS	Attainable Moment Set
CA	Control Allocation
DA	Direct Allocation
CCoP	Control Center of Pressure
CG	Center of Gravity
DLC	Direct Lift Control
FCS	Flight Control System
ICR	Instantaneous Center of Rotation
LAMS	Largest Attainable Moment Set
NDI	Non-linear Dynamic Inversion
PI	Pseudo Inverse
PrP	PrandtlPlane
RMS	Root Mean Squared
WPI	Weighted Pseudo Inverse

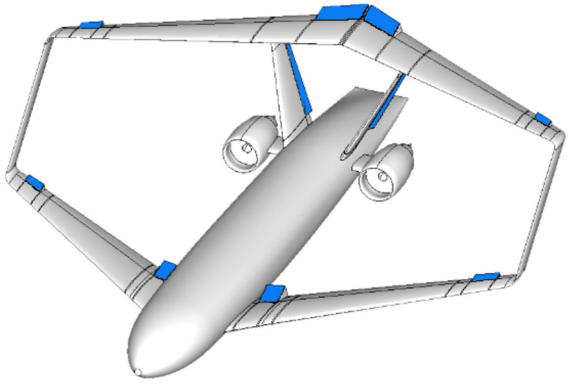

Fig. 1. The Prandtlplane aircraft configuration with deflected control surfaces.

the aerodynamic forces generated solely by displacing the aircraft control effectors. Without focusing on any specific aircraft configuration or practical implementation of DLC, the derivation in [11] shows the theoretical variation of the load factor time response as a function of the position of CCoP. For example, conventional pitch control, obtained with a single control force very far aft the aircraft Center of Gravity (CG), is characterized by the CCoP roughly coinciding with the location of the control effector itself. As the CCoP moves fore of the aircraft aerodynamic center, the initial and steady-state load factor responses are concordant in sign. In particular, if the CCoP is fore of the aerodynamic center by the same distance the maneuver point is aft of the CG, the load factor steady-state response is theoretically equal to the initial one. This is referred to as "Pure DLC" [11], since the capability to generate lift with angle of attack dynamics is not exploited in this case.

In the most extreme case of Pure DLC, it should be easy to understand how enabling this control technique would allow the pilot to have precise and almost instantaneous control of the aircraft lift. Even if at the cost of limited control power, DLC can then be beneficial in all flight scenarios that require maneuver accuracy and response quickness, such as precision landing or obstacle avoidance tasks, for example.

Existing applications of some forms of DLC can be traced to the use of spoilers and flaps [12–14], although the latter cannot be used as control effectors and hence have no role in maneuvering flight. With a more original approach, an interesting research study evaluates DLC performance by means of classic and newly proposed handling qualities criteria, for two conventional aircraft models, as a function of the gearing ratios used to gang control effectors together [15].

Gearing and ganging control effectors is the most straightforward way to constrain their relative motion. This clearly has an impact on the position of the CCoP, and hence on the type of transient response that can be achieved in maneuvering flight. On the other hand, gearing ratios and ganging matrices need to be selected *a priori* and somewhat arbitrarily, and usually need to be optimized for different flight scenarios. This clearly hinders the potential range of achievable aircraft dynamic responses.

A more advanced approach to calculate the control effectors position required to perform a given maneuvering task is represented by Control Allocation (CA) methods [16]. These methods exploit the aerodynamic effectiveness of each effector to achieve a given control objective while satisfying some assigned optimality criterion. Among the many CA formulations available in literature, two well-known approaches, with very different characteristics and performance, are the Weighted Pseudo Inverse (WPI) method and the Direct Allocation (DA) method.

Table 1
Top-level design parameters of the PrandtlPlane.

b	36.0 m
$\overline{c}$	4.31 m
S	266.7 m^2
h_{cr}	11 km
M_{cr}	0.79
N_{pax}	308
m_{MTO}	122 $\times$ 10^3 kg

Many research works have already focused on evaluating the practical implications of performance differences between these, and other, CA algorithms. A detailed evaluation of the numerical performance of four classic formulations is presented in [17]. A comprehensive study, relying on a high-fidelity wind-tunnel database for a Blended Wing Body aircraft model, estimates the impact of classic CA methods on trim drag and control surface design [18,19]. A recent, innovative research work defines and exploits the concept of robust Attainable Moment Set (AMS), with applications to fighter aircraft with uncertainties in their control effectiveness [20]. In light of its independence from any iterative procedure, the WPI method has been implemented in a distributed CA scheme for spacecraft attitude stabilization [21]. Several research studies have also proposed modifications of classic CA methods to solve specific engineering problems: from a multi-step DA method to minimize drag [22], to the inclusion of aerodynamic interactions among the effectors [23]; from a multi-objective CA formulation aimed at minimizing structural loads due to control efforts [24], to gust load alleviation by means of CA of the lift and pitch moment coefficients [25].

The objective of the present work is to develop a CA formulation which is able to alter the dynamic transient response of an aircraft. This is achieved for a given Flight Control System (FCS) architecture and, optionally, tuning, by exclusive means of the aerodynamic effectiveness of the aircraft control effectors.

The following Section 2.1 starts by illustrating the aircraft and flight mechanics model implemented for the present study. Section 2.2 goes into more detail on the employed FCS architecture, as well as on the procedure implemented to tune it. A brief technical overview of the classic CA problem is then outlined in Section 2.3, and the proposed novel CA formulation is then presented in Section 2.4. Three relevant application studies are presented in Section 3, with results and discussion. Lastly, conclusions are drawn in Section 4, with an outlook on future research possibilities.

2. Methodology

2.1. Aircraft model

The PrP concept under consideration in the present article has been designed for short and medium range flights within the PARSIFAL (Prandtlplane ARchitecture for the Sustainable Improvement of Future AirpLanes) research project. Some relevant design parameters are reported in Table 1.

Its aerodynamic characteristics have been obtained using the commercial off-the-shelf panel code VSAERO [26]. Each of the aerodynamic forces and moments acting on the aircraft is expressed as a tabular function of flight parameters and control surface deflections $\boldsymbol{\delta}$. The resulting aerodynamic model, assuming partial superposition of effects, is reported in Equation (1).

$$C_{\boldsymbol{\mathcal{M}}} = \underbrace{C_{\boldsymbol{\mathcal{M}}_0}(\alpha, \beta, M, \boldsymbol{\delta} = \mathbf{0})}_{\text{steady, clean}} + \underbrace{\sum_{i=1}^{N_\delta} \Delta C_{\boldsymbol{\mathcal{M}}}(\alpha, \beta, M, \delta_i)}_{\text{steady, control effectors}} + \underbrace{\sum_{\omega=p,q,r} C_{\boldsymbol{\mathcal{M}}_\omega}(\alpha, \beta, M, \boldsymbol{\delta} = \mathbf{0})\, \omega}_{\text{unsteady, clean}} \tag{1}$$

The propulsive model of its two engines has been generated with an in-house, physics-based, simulation toolbox [27]. It expresses thrust and fuel consumption as a tabular function of altitude, Mach number and throttle, and has been validated in a previous study about mission performance of the PrP [8].

Together with a FCS architecture, which is described in more detail in the following section, the aerodynamic, propulsive and mass databases are merged into a consistent flight mechanics model, within the framework of the Performance, Handling Qualities and Load Analysis Toolbox (PHALANX). This software suite, written in MATLAB® and Simulink®, revolves around a Simscape Multibody Dynamics core to perform non-linear flight simulations. It relies on a modular, physics-based and configuration-agnostic architecture, which is able to operate consistently with different levels of input fidelity. Thanks to ts capability to support automatic aircraft design workflows, PHALANX has been used in a number of research studies and applications on different aircraft configurations [8–10,28–31]. A block-scheme overview of the toolbox is shown in Fig. 2.

For the present study, symmetric flight has been imposed by constraining the aircraft model to have only three degrees of freedom in the vertical plane. The normal load factor in body axes has been defined as

$$n_{z_B} = -\frac{\sum Z_B}{mg} \tag{2}$$

in order to have $n_{z_B} \approx 1$ in straight and level flight.

2.2. Flight Control System architecture

The implemented FCS architecture is reported in Fig. 3. It consists of a simple airspeed hold, employing the throttle command, and a longitudinal control law based on Non-linear Dynamic Inversion (NDI). The latter technique allows to neatly separate the control law from the CA components, and to use classic methods from linear control theory for tuning the controller gains. Control inputs for the latter are provided either from the pilot stick, with a pitch rate response type, or from an altitude controller.

The altitude channel employs a series of linear controllers and transformations to achieve stable and robust augmented dynamics [32]. The transformation between the reference vertical acceleration $\ddot{h}_{des}$ and the normal load factor assumes there is no variation in airspeed and is expressed in Equation (3).

$$\ddot{h} = g\left(n_{z_B}\cos\theta - 1\right) \tag{3}$$

The transformation between the load factor and the desired angle of attack α_{des} makes use of the linear approximation of the lift curve in body axes at trim conditions, and is reported in Equation (4). The commanded angle of attack is clipped between -5 deg and 5 deg to prevent the run-time values of α from exceeding the boundaries of the underlying aerodynamic dataset.

$$q_\infty S\left[C^{tr}_{Z_0} + C^{tr}_{Z_\alpha}\left(\alpha - \alpha^{tr}\right)\right] = -mgn_{z_B} \tag{4}$$

Lastly, the transformation between the reference angle of attack rate $\dot{\alpha}_{des}$ and the commanded pitch rate q_{cmd} is expressed in Equation (5).

$$q = \dot{\alpha} - \frac{g}{V}\left(\cos\theta - n^{tr}_{z_B}\right) \tag{5}$$

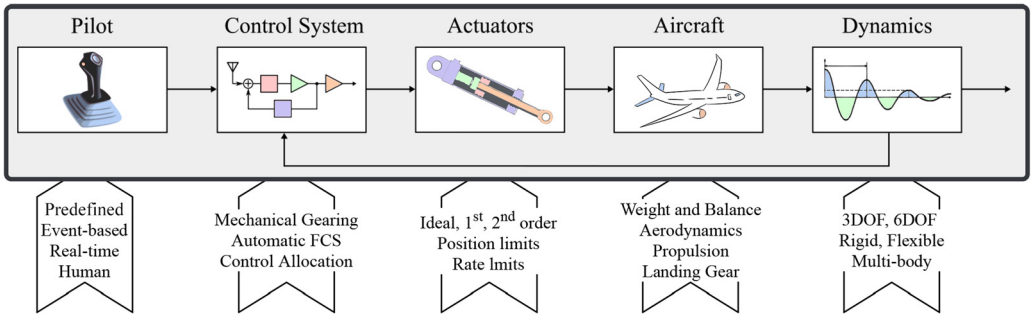

Fig. 2. Block-scheme overview of PHALANX.

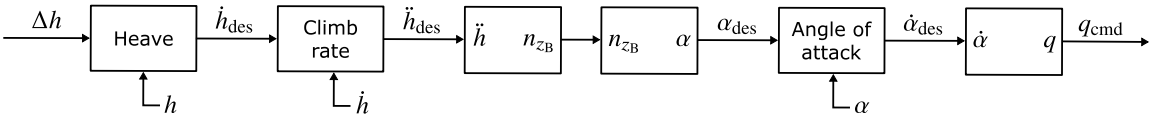

a) Altitude control channel

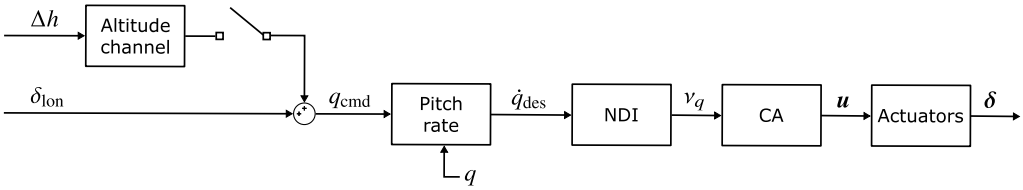

b) Main flight control law

Fig. 3. Block scheme overview of the chosen FCS architecture.

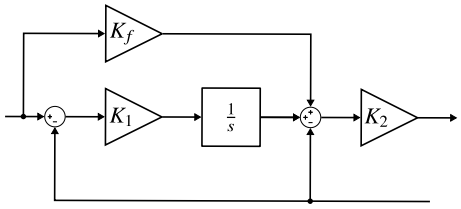

Fig. 4. Baseline architecture for all controllers shown in Fig. 3.

Each of the controllers shown in Fig. 3 has the baseline architecture reported in Fig. 4, consisting of two cascaded proportional-integral control loops, with a parallel feedthrough branch for improved tracking response [32]. For each controller, the feedthrough gain fraction K_f is assigned manually in order to obtain desired closed-loop characteristics. The proportional gains K_1 and K_2 are left to be determined by an automatic tuning procedure. This is formulated as an optimization problem, with the objective to find the values of the proportional gains that minimize the difference between the closed-loop dynamics of the linear aircraft model and an assigned reference model. Without loss of generality, the latter has been arbitrarily chosen as follows:

- the reference altitude dynamics is a critically damped second order system with a time constant of 2 s;
- the reference airspeed dynamics is a first order system with a time constant of 3 s.

The proprietary Control System Tuner algorithm by MathWorks® has been used to solve the optimization problem and find the tuned values of the gains for every case study presented in the present paper.

In the case of symmetric flight with three-degrees of freedom, the classic NDI of aircraft rotational dynamics resolves to the simple scalar equation reported in Equation (6), where ν_q is the non-dimensional pitch control moment required to obtain the desired pitch acceleration $\dot{q}_{\text{des}}$.

$$J_{yy}\dot{q}_{\text{des}} = \frac{\mathcal{M}^{\text{tr}}}{q_\infty S\bar{c}} + \nu_q \tag{6}$$

The pitch control moment ν_q, together with null control moments about the roll and yaw axes, is then allocated to the effectors by solving an appropriate CA problem based on Equation (7).

$$B\boldsymbol{u} = \boldsymbol{\nu} \quad \Leftrightarrow \quad \begin{bmatrix} B^{\mathcal{L}} \\ B^{\mathcal{M}} \\ B^{\mathcal{N}} \end{bmatrix} \boldsymbol{u} = \begin{Bmatrix} 0 \\ \nu_q \\ 0 \end{Bmatrix} \tag{7}$$

The notation, explained in the following Equation (8), has been chosen to highlight to contribution of each row of the B matrix, and is going to be used in the next section, covering the proposed CA formulation.

$$B^H = \begin{bmatrix} \frac{\partial C_H}{\partial u_1} & \frac{\partial C_H}{\partial u_2} & \cdots & \frac{\partial C_H}{\partial u_n} \end{bmatrix} \qquad \text{for } H = \mathcal{L}, \mathcal{M}, \mathcal{N} \tag{8}$$

2.3. Overview of the classic Control Allocation problem

The baseline, generic CA problem consists in finding the value of the control effectors displacements $\boldsymbol{u}$ which solves the following Equation (9).

$$B\boldsymbol{u} = \boldsymbol{\nu} \tag{9}$$

In this simple relation, $\boldsymbol{\nu}$ is a vector of objectives to be achieved by means of displacement of the control effectors $\boldsymbol{u}$. Reference values for $\boldsymbol{\nu}$ are typically prescribed by the FCS and can represent control forces and moments or rotational rates, in the most common applications. B is the control effectiveness matrix, which is not square

and cannot be inverted in case of redundant effectors. CA methods define an analytic or algorithmic function f, which allows to express the control effectors displacements as

$$\boldsymbol{u} = f(B, \boldsymbol{v}, \dots). \tag{10}$$

The WPI method finds the required effectors displacements by solving the following optimization problem:

$$\begin{aligned} \min_{\boldsymbol{u}} \quad & \|W_{\boldsymbol{u}}(\boldsymbol{u} - \boldsymbol{u}_{\text{des}})\|^2 \\ \text{s.t.} \quad & B\boldsymbol{u} - \boldsymbol{v} = 0 \end{aligned} \tag{11}$$

where $W_{\boldsymbol{u}}$ is a weighting matrix used to prioritize the effectors, and $\boldsymbol{u}_{\text{des}}$ is a preferred effectors displacement. This formulation admits the following analytic solution [16]

$$\boldsymbol{u} = \boldsymbol{u}_{\text{des}} + W_{\boldsymbol{u}}^{-1} B^T \left(B W_{\boldsymbol{u}}^{-1} B^T \right)^{-1} (\boldsymbol{v} - B\boldsymbol{u}_{\text{des}}) \tag{12}$$

which makes the WPI method very robust in every application. However, this comes at the price of sub-optimal allocation performance, as the AMS of the WPI method is significantly less extended than the aircraft Largest Attainable Moment Set (LAMS) [33]. This means that a large set of prescribed objectives $\boldsymbol{v}$, which would be theoretically achievable in light of the control effectiveness of the aircraft B, are not practically attainable, because the WPI algorithm is not capable of mapping them to an admissible set of control effectors positions $\boldsymbol{u}$.

On the other hand, the DA method relies on the geometric representation of the AMS itself, and is hence capable of achieving all of the prescribed objectives within the LAMS [33]. DA is usually formulated as the optimization problem shown in Equation (13), making use of the auxiliary variable $\boldsymbol{w} \equiv \boldsymbol{u}$.

$$\left.\begin{aligned} \max_{\rho, \boldsymbol{w}} \quad & \rho \\ \text{s.t.} \quad & B\boldsymbol{w} = \rho \boldsymbol{v} \\ & \boldsymbol{u}_{\min} < \boldsymbol{w} < \boldsymbol{u}_{\max} \end{aligned}\right\} \Rightarrow \begin{cases} \boldsymbol{u} = \boldsymbol{w}/\rho, & \text{if } \rho > 1 \\ \boldsymbol{u} = \boldsymbol{w}, & \text{if } \rho \leq 1 \end{cases} \tag{13}$$

In its most computationally efficient formulation, DA is cast as a Linear Programming problem, hence relying on an iterative algorithm for its solution [17]. The DA formulation takes into account effectors saturation limits and preserves direction in Moment Space for unattainable desired moments [33], but does not allow any prioritization of effectors via weighting matrices.

2.4. Novel Control Allocation formulation

The novel CA formulation revolves around the mathematical definition of the CCoP. In the scope of symmetric flight in a vertical plane, its non-dimensional longitudinal position in body axes is calculated as in Equation (14) [11].

$$\overline{x}_\delta = \frac{x_\delta}{\overline{c}} = -\frac{\sum_{i=1}^{N_\delta} \Delta C_{\mathcal{M}_i}}{\sum_{i=1}^{N_\delta} \Delta C_{Z_i}} \approx -\frac{\sum_{i=1}^{N_\delta} C_{\mathcal{M}_{\delta_i}} \delta_i}{\sum_{i=1}^{N_\delta} C_{Z_{\delta_i}} \delta_i} = -\frac{B^{\mathcal{M}}\boldsymbol{\delta}}{B^Z \boldsymbol{\delta}} \tag{14}$$

For an alternative interpretation of this quantity from a flight dynamics perspective, it is useful to elaborate on the previous expression in the case of a single control surface, e.g. an elevator. In this case, $\overline{x}_\delta$ can be simply expressed as the ratio between the pitch moment and normal force control derivatives, and coincides with the position of the elevator itself. Additionally, it is also strictly related to the Instantaneous Center of Rotation (ICR) of the aircraft, which is calculated as in Equation (15) in the scope of a linear dynamic formulation [34].

$$\overline{x}_{\text{icr}} = \frac{J_{yy}}{m\overline{c}^2} \frac{C_{Z_{\delta_e}}}{C_{\mathcal{M}_{\delta_e}}} = -\frac{J_{yy}}{m\overline{c}^2} \frac{1}{\overline{x}_\delta} \tag{15}$$

In light of this, it should be evident how the position of the CCoP is capable to substantially affect the flying qualities of the aircraft in the pitch axis [35]. For a linear dynamic model, it can be derived from the previous equation that the product between the positions of the CCoP and the ICR must be constant. If the elevator is very far aft of the aircraft CG, the ICR falls relatively close to it. In other words, the impact of the normal control force is negligible when compared to the pitch control moment, and the aircraft motion resembles a pure rotation about its CG. On the other hand, if the CCoP tends to the aircraft CG, the ICR moves infinitely away from it, and the aircraft motion tends to a pure normal translation.

These types of deductions, obtained in the simplified case of a single control effector and linear dynamics, motivate the effort presented in the current paper. The objective of the present investigation is to shape the transient response of the aircraft by means of CA methods. This is achieved by driving the CCoP towards a prescribed reference location $\overline{x}_{\text{ref}}$, for which the transient response is known to have desired characteristics, and translates into the following Equation (16).

$$\overline{x}_\delta = -\frac{B^{\mathcal{M}}\boldsymbol{\delta}}{B^Z\boldsymbol{\delta}} \to \overline{x}_{\text{ref}} \;\Leftrightarrow\; \frac{\left(B^Z\overline{x}_{\text{ref}} + B^{\mathcal{M}}\right)\boldsymbol{\delta}}{B^Z\boldsymbol{\delta}} \to 0 \tag{16}$$

Assuming that there exists at least a combination of $\overline{x}_{\text{ref}}$ and $\boldsymbol{\delta}$ which verifies this limit, i.e. that control effectors can physically drive the CCoP to its desired location, Equation (16) becomes an equality. Furthermore, for any realistic maneuvering scenario, i.e. assuming that $\boldsymbol{\delta} \neq \boldsymbol{0}$, the latter reduces to its numerator as shown in Equation (17).

$$\left(B^Z\overline{x}_{\text{ref}} + B^{\mathcal{M}}\right)\boldsymbol{\delta} = 0 \tag{17}$$

The last equation can be re-written in matrix form as

$$\begin{bmatrix} \overline{x}_{\text{ref}} & 1 \end{bmatrix} \begin{bmatrix} B^Z \\ B^{\mathcal{M}} \end{bmatrix} \boldsymbol{\delta} = XB^*\boldsymbol{\delta} = 0 \tag{18}$$

where $X = [\overline{x}_{\text{ref}}\ 1]$ and $B^* = \begin{bmatrix} B^Z & B^{\mathcal{M}} \end{bmatrix}^T$.

From a geometric point of view, Equation (18) identifies a hyperplane in Control Space, which passes through the origin, and whose orientation depends on the value of $\overline{x}_{\text{ref}}$. This linear constraint obviously maps to a much smaller AMS than the one obtained when all effectors are free to move independently. From a more technical standpoint, Equation (18) can be regarded in two alternative ways, which give life to two different approaches to exploit it.

2.4.1. Control effectiveness matrix augmentation

The first, and probably most straightforward, approach sparks out of the interpretation of Equation (18) as a CA problem itself, where the prescribed objective is equal to zero, and the desired position of the CCoP acts as a weight to prioritize the generation of control lift over control pitch, or vice-versa. The combined effectiveness XB^* can then be used to augment the B matrix of any standard CA problem formulation, as shown in the following Equation (19).

$$B\boldsymbol{u} = \boldsymbol{v} \longrightarrow \begin{bmatrix} B \\ XB^* \end{bmatrix} \boldsymbol{u} = \begin{Bmatrix} \boldsymbol{v} \\ 0 \end{Bmatrix} \tag{19}$$

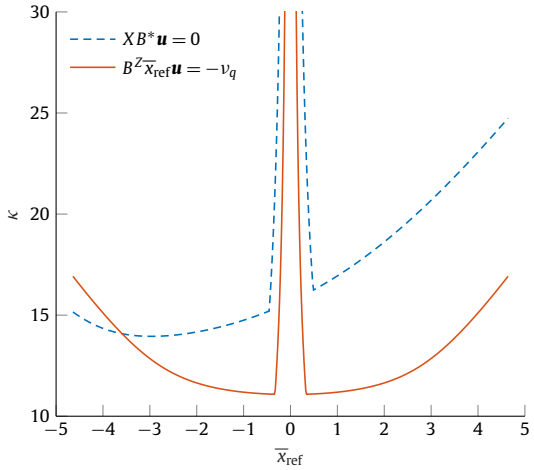

Fig. 5. Condition number of the augmented control effectiveness matrix, for two augmentation approaches.

In this way, Equation (18) has been directly injected into the CA problem, and has been given the same dignity as the other equations for the allocation of prescribed objectives. This approach can be applied to any existing CA method, including DA, as it only needs the presence of a baseline control effectiveness matrix in the problem formulation.

On the other hand, this approach presents a major drawback: the condition number κ of the augmented effectiveness matrix increases abruptly as the CCoP tends to the aircraft CG, until diverging completely at the latter position. This is due to the fact that the pitch moment row $B^{\mathcal{M}}$ and the extra row XB^* of the augmented effectiveness matrix become more and more similar as $\overline{x}_{\text{ref}}$ approaches zero. From a physical point of view, this happens because the pitch effectiveness of the control effectors is used to allocate both the demanded pitch moment ν_q and the null extra objective required to prioritize the effectors.

The numerical conditioning of the augmented effectiveness matrix can be slightly improved by additionally assuming that the CA algorithm always converges, i.e. that the equality for the pitch moment $B^{\mathcal{M}}\boldsymbol{u}=\nu_q$ is verified at all times. This is not true for commanded control moments outside of the AMS, for example. With this additional hypothesis, Equation (17) can be re-written as in Equation (20), and the augmented problem takes the shape presented in Equation (21).

$$B^Z\overline{x}_{\text{ref}}\boldsymbol{u}=-\nu_q \tag{20}$$

$$B\boldsymbol{u}=\boldsymbol{\nu}\longrightarrow\begin{bmatrix}B\\B^Z\overline{x}_{\text{ref}}\end{bmatrix}\boldsymbol{u}=\begin{Bmatrix}\boldsymbol{\nu}\\-\nu_q\end{Bmatrix} \tag{21}$$

As shown in Fig. 5, also in this case the augmented effectiveness matrix becomes ill-conditioned for $\overline{x}_{\text{ref}}\rightarrow 0$. In light of this, this approach would not be suitable for any practical implementation of the proposed CA formulation. It is therefore not implemented in any of the applications presented in the remainder of this paper. The more robust weighted prioritization method illustrated in the next section does not present any numerical instabilities, and has been used to obtain the results presented in the remainder of the article.

2.4.2. Weighted prioritization

Equation (18) can also be interpreted as a particular case of the classic effector prioritization expression, shown in the following Equation (22), used in all CA methods based on quadratic-programming algorithms.

$$XB^*\boldsymbol{u}\quad\Leftrightarrow\quad W_{\boldsymbol{u}}\left(\boldsymbol{u}-\boldsymbol{u}_{\text{des}}\right) \tag{22}$$

The equivalence can be easily achieved by imposing the preferred effectors position as null, and placing the combined effectiveness vector on the diagonal of the weighting matrix, as shown in Equation (23).

$$\boldsymbol{u}_{\text{des}}=0\qquad W_{\boldsymbol{u}}=\text{diag}\left(XB^*\right) \tag{23}$$

This approach does not present any numerical conditioning issues. On the other hand, it can only be applied to CA problems which allow some form of effectors prioritization, such as those employing the WPI method. In case $\overline{x}_{\text{ref}}$ coincides with the CG, control effectors are simply prioritized according to their pitch moment effectiveness $B^{\mathcal{M}}$.

A WPI method based on this particular formulation is going to be employed for all the applications proposed in the following Section 3. The control surface deflections solving such CA problem are obtained by substituting the expressions reported in Equation (23) into Equation (12).

3. Applications and results

Three study cases have been performed to explore the flight mechanics possibilities of the PrP. In all cases, the performance of the novel CA formulation presented in the previous Section 2.4.2 is evaluated as a function of the prescribed position of the CCoP and compared against the standard Pseudo Inverse (PI) formulation. The latter is simply equivalent to the WPI approach with the effectors not being weighted, i.e. $W_{\boldsymbol{u}}=I$.

As explained in the next section, the aircraft is trimmed using an iterative methodology based on DA and the concept of AMS. For all the subsequent applications, the control effectiveness matrix B is calculated at trim conditions and is held constant throughout each flight simulation. Actuators are modeled as first order systems with a time constant of 0.1 s and a rate limit of ± 45 deg/s. Control surface deflections are saturated at ± 30 deg. The FCS is re-tuned for each prescribed value of $\overline{x}_{\text{ref}}$, using the automatic procedure described in Section 2. However, if the FCS is tuned using the standard PI method and then left unaltered when using the modified CA approach, results are substantially not affected and conclusions unhindered.

The reference trim condition is briefly illustrated in the following Section 3.1. Section 3.2 presents a simple pull-up maneuver with detailed analysis of time histories of the normal load factor and control surface deflections. In Section 3.3, an altitude tracking maneuver is analyzed. This is performed by closing the altitude channel switch in Fig. 3b and prescribing a reference altitude profile. In a similar fashion, Section 3.4 presents an altitude holding task in turbulent atmosphere, with the estimation of a quantitative index of the comfort level on board.

3.1. Trim condition

The aircraft model is trimmed in straight and level flight using the CA-based methodology presented in [10]. With this approach, the resulting control surface deflections are not constrained by an imposed ganging and gearing kinematic chain, but are independently set to obtain the maximum balanced control authority about the lift and pitch axes. The standard DA method of Equation (13) is used in this case, because of its properties concerning the AMS. The Linear Programming formulation provided by [17] is implemented. The AMS geometry at trim, and the combination of trim control forces generated by the effectors are shown in Fig. 6a. Trim control surface deflections are reported in Fig. 6b. The aircraft is trimmed at $V^{\text{tr}}=170$ m/s at sea level altitude.

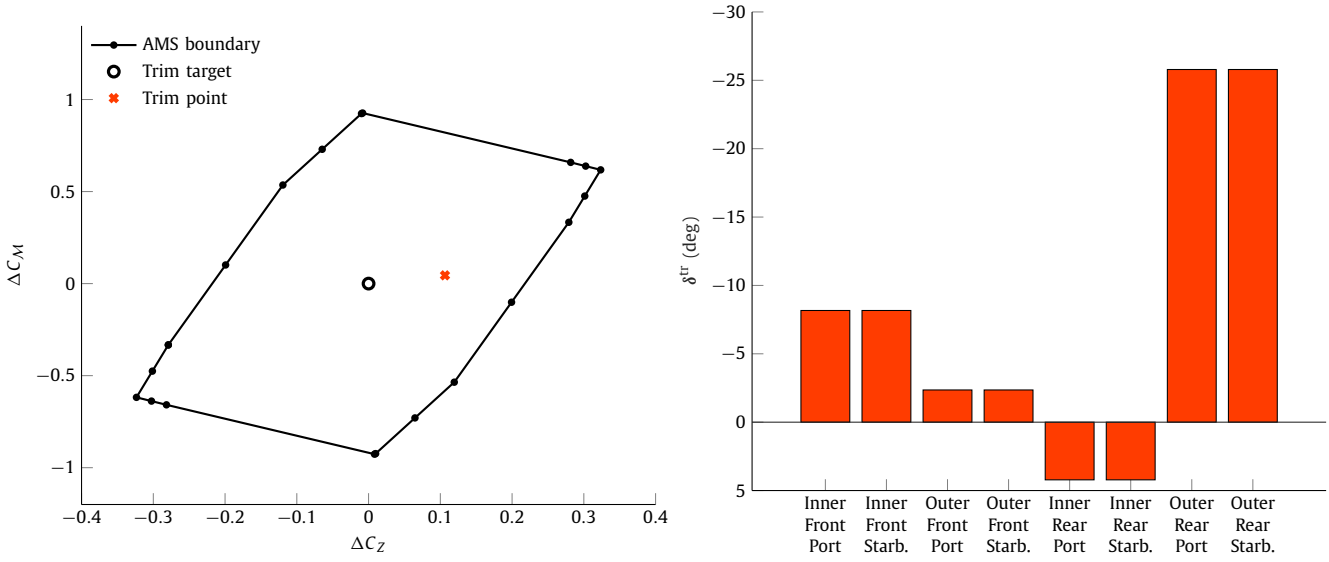

a) Control forces and AMS geometry **b)** Control surface deflections

Fig. 6. Reference trim condition: $V^{tr} = 170$ m/s, $\alpha^{tr} = -0.46$ deg. Control surface deflections are bounded in the $[-30, +30]$ deg interval.

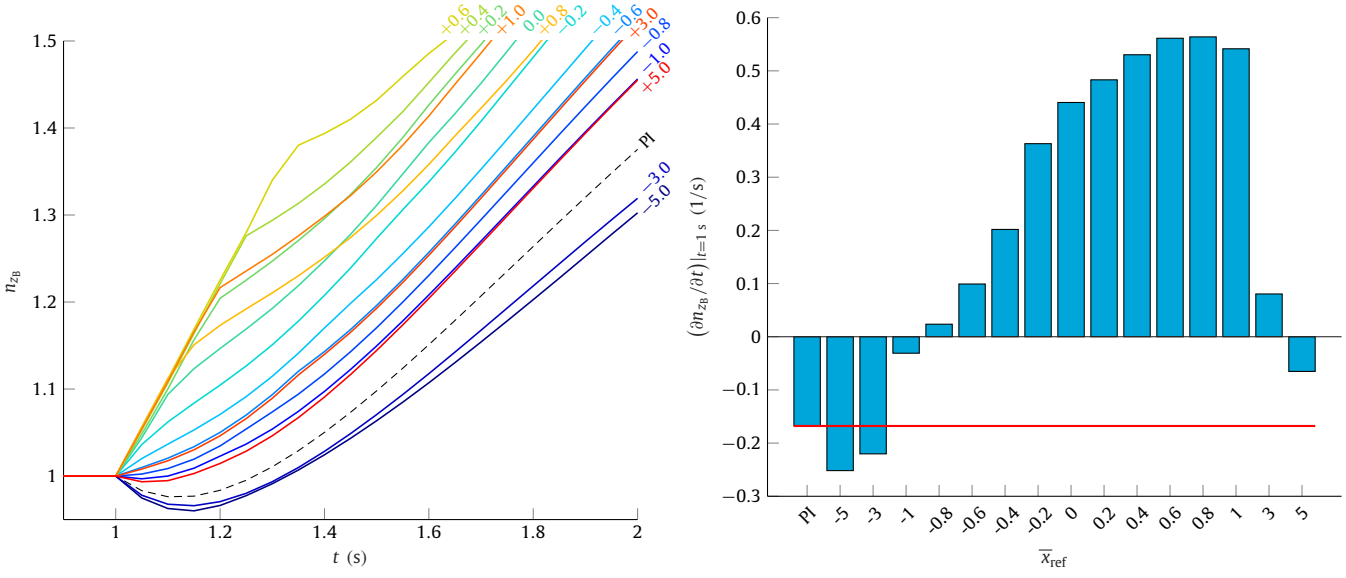

a) Time histories **b)** Time derivative at $t = 1$ s

Fig. 7. Normal load factor response after an impulsive pull-up maneuver, for different values of the reference CCoP location and the standard PI approach.

Trim control surface deflections, positive if with trailing edge down, are all symmetric and contained in magnitude, apart from the outboard ones on the rear wing, which are partially sacrificed to obtain a very small trim angle of attack $\alpha^{tr} = -0.46$ deg. Rudders have been explicitly excluded from the CA problem, as they have a significant cant angle which makes them suitable for pitch control as well. This was judged to be undesired in a conventional flight control scenario.

3.2. Pull-up maneuver

A step pull-up maneuver is performed by prescribing a constant pitch rate command through the pilot longitudinal control channel δ_{lon}, for the duration of 10 s, with the altitude channel switch left open, as shown in Fig. 3b. The initial instants of the arising load factor response are reported in Fig. 7a, for several values of $\overline{x}_{ref}$ and the standard PI formulation. Similarly, the time derivative of the load factor response at the start of the pilot maneuver is reported in Fig. 7b and used as an indication of the sharpness of the transient response.

The standard PI method results in the typical non-minimum phase behavior of conventional aircraft configurations. Such response corresponds to a CCoP far aft the aircraft CG, which would be equivalent, in the modified CA formulation, to a value of $\overline{x}_{ref}$ approximately equal to -2. A similar behavior is observed with the modified CA approach, for values of $\overline{x}_{ref}$ ranging from -5 to about -0.9.

By advancing the prescribed location of the CCoP, i.e. increasing the value of $\overline{x}_{ref}$ from -5 to about 0.8, the initial decrease in load factor is progressively reduced, neutralized and converted into a sharp initial increase. The maximum response sharpness appears to plateau for $0.4 < \overline{x}_{ref} < 1$, where the transient response clearly shows the typical characteristics of DLC [11]. By further increasing $\overline{x}_{ref}$, the trend is reversed, and for $\overline{x}_{ref} = 5$ a small initial decrease in the load factor is again observed.

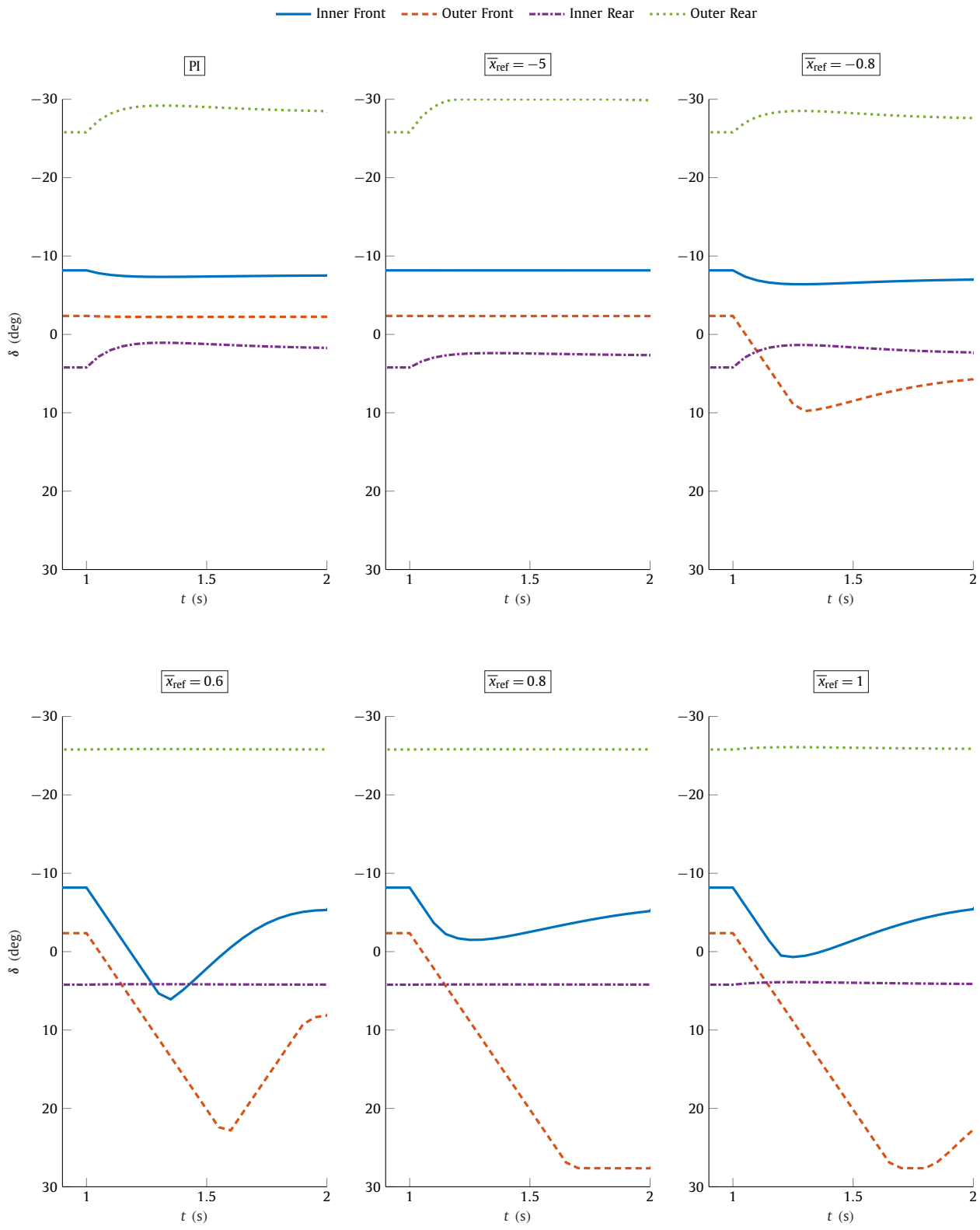

Fig. 8. Control surface deflections time histories after an impulsive pull-up maneuver, for different values of the reference CCoP location and the standard PI approach.

These results are consistent for different amplitudes and durations of the commanded input, which may be representative of different levels of pilot aggressiveness in performing the maneuver. In this specific application, for $0 < \overline{x}_{ref} < 1$, the aircraft response is so sharp that the commanded pitch rate is achieved before the end of the pilot maneuver. This forces control surfaces to be deflected abruptly back, to some extent, before reaching a steady state value, and results in the acceleration cusp visible in the corresponding curves of Fig. 7a.

The time histories of control surface deflections are shown in Fig. 8 for notable values of $\overline{x}_{ref}$. First, it can be seen how the standard PI allocation mainly relies on the use of control surfaces

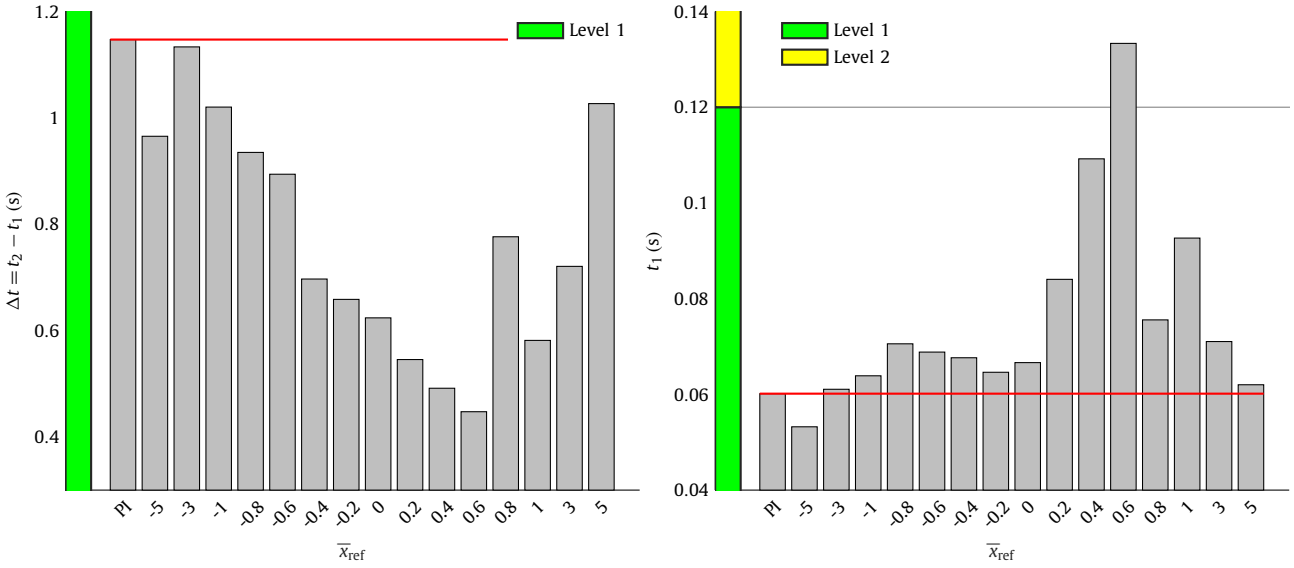

a) Rise time **b)** Equivalent time delay

Fig. 9. Time-domain flying qualities of the short period pitch rate response q, for different values of the reference CCoP location and the standard PI approach.

on the rear wing. As expected, both the inner and outer rear effectors are deflected upwards in order to perform the prescribed pull-up maneuver, while the inner front effectors are only slightly activated downwards. This is in light of their lower pitch effectiveness, which is due to their smaller distance to the aircraft CG w.r.t. their counterpart on the rear wing. The outer front effectors are left completely untouched.

Similar observations hold for the modified approach, in the case of $\overline{x}_{ref} = -5$. Such high, negative value places even more emphasis on the rear wing effectors, and in particular on their lift effectiveness. In fact, outer rear effectors are now prioritized w.r.t. inner ones, since they are closer to the CG and their pitch effectiveness is lower. The former are deflected upwards until saturation, while the latter are now deflected less than in the previous case. All front effectors are unused.

In the case of $\overline{x}_{ref} = -0.8$, all effectors are used in a balanced way, resulting in a smooth initial load factor response. Front effectors are deflected downwards, while rear effectors are deflected upwards, so that the combined deflection generates a pure torque about the aircraft CG, and the maneuver is substantially started by α-generated lift.

For $0.6 < \overline{x}_{ref} < 1$, all the control effort is placed on front effectors, while rear ones are almost completely ignored. Both inner and outer effectors on the front wing are deflected significantly downwards, with the outer ones exhibiting larger deflections in light of their smaller effectiveness. For $\overline{x}_{ref} = 0.8$, inner effectors are deflected less than in the case of $\overline{x}_{ref} = 0.6$, while outer ones are deflected up almost to the saturation limit. Both $\overline{x}_{ref} = 0.6$ and $\overline{x}_{ref} = 0.8$ result in the highest response sharpness for the present application, with the former value being able to obtain a larger initial load factor excursion thanks to the more substantial use of inner front effectors.

For $\overline{x}_{ref} = 1$, inner front effectors are deflected more than in the case of $\overline{x}_{ref} = 0.8$, outer front effectors reach the same final value as in the previous case, while a very slight upward deflection of all the rear effectors is once again noticeable. By further advancing the reference CCoP location, control effectors deflections result similar to the ones obtained for the $\overline{x}_{ref}$ negative value that exhibits a similar response, e.g. $\overline{x}_{ref} = -0.6$ and $\overline{x}_{ref} = 3$, or $\overline{x}_{ref} = -1$ and $\overline{x}_{ref} = 5$, as shown in Fig. 7a.

The rise time and equivalent time delay of the pitch rate response are shown in Fig. 9. These are two classic flying qualities metrics, used to characterize the short period pitch rate response of the aircraft to pilot commands [35]. Time delay t_1 is defined as the lapse between the step command and the instant when the tangent line at the maximum pitch rate slope intersects the time axis. Rise time $\Delta t = t_2 - t_1$ is defined as the lapse between t_1 and the instant when the maximum pitch rate slope line intersects the steady state value of the pitch rate for the first time. For the presented application, these metrics have been evaluated on the basis of non-linear flight dynamics simulations.

As it can be seen in the figure, the metrics show a somewhat complementary behavior as a function of $\overline{x}_{ref}$. For basically all values of $\overline{x}_{ref}$, the modified CA approach determines a consistent improvement of the rise time with respect to the standard PI method. All values are well within the Level 1 flying quality rating, and the minimum rise time is achieved for $\overline{x}_{ref} = 0.6$. On the other hand, a slight deterioration of the time delay can be seen for nearly all values of $\overline{x}_{ref}$, with a peak increase for $\overline{x}_{ref} = 0.6$. The latter is the only case for which the flying quality criterion results in a Level 2 rating.

The selected metrics are deemed appropriate to characterize the dynamic behavior of the augmented aircraft model, although the criteria which prescribe their limit values have been developed for more conventional aircraft configurations. In particular, concerning their suitability for the present application, it must be reported that "several questions remain unresolved [...]. Effects of pilot location and blended direct lift control have been observed and need to be accounted for" [35]. This may constitute the object of interesting future research studies.

3.3. Altitude shift maneuver

The present application has the objective of estimating the impact of the modified CA approach on a practical performance metric such as tracking precision. A 10 m square wave altitude profile $h_{ref}(t)$ is prescribed for the aircraft to track. This is achieved by closing the altitude channel switch in Fig. 3b and leaving the pilot input unaltered. The resulting altitude time histories are reported in Fig. 10 for different values of $\overline{x}_{ref}$ and the standard PI approach.

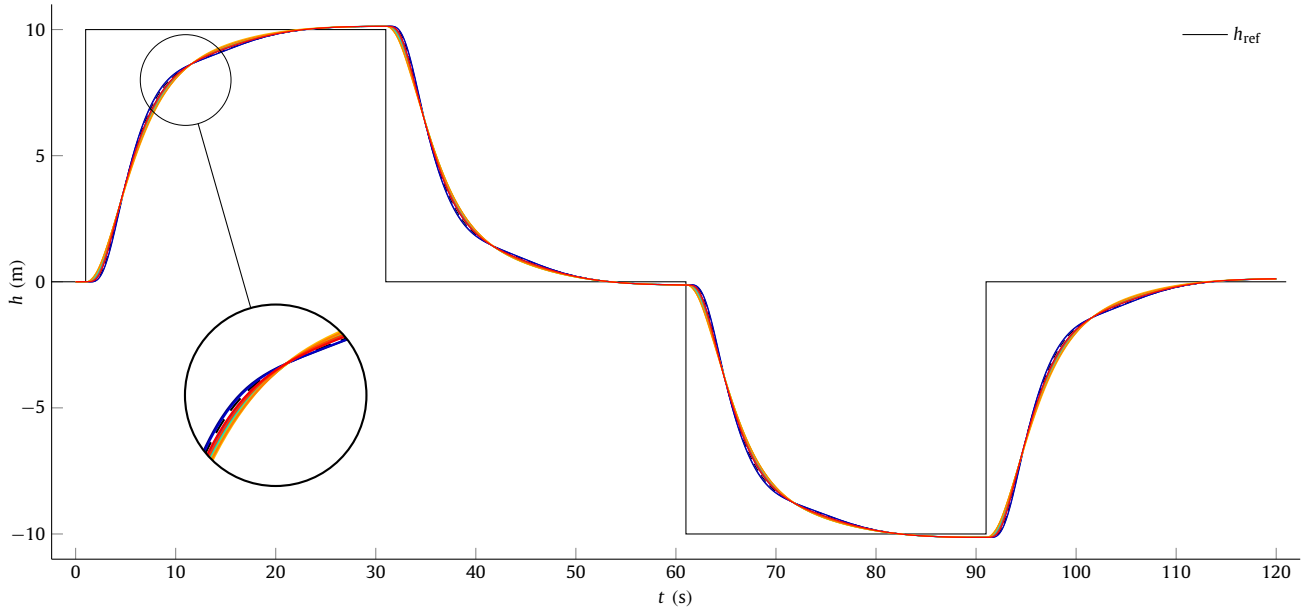

Fig. 10. Altitude time histories for the altitude shift task, for different values of the reference CCoP location and the standard PI approach. Trajectories are fundamentally indistinguishable and therefore have not been labeled individually.

Apart from a very small difference during climb and descent phases, the trajectories are basically indistinguishable at the scale of the full maneuver duration. This is also in light of the fact that the FCS is re-tuned for every value of $\overline{x}_{ref}$, using the same performance requirements within the automatic procedure presented in Section 2.

Nevertheless, the alteration of the dynamic response achieved with the modified CA approach has a small but noticeable impact on trajectory tracking precision. The Root Mean Squared (RMS) deviation $\overline{\Delta h}$ of each altitude time history w.r.t. the reference one is reported in Fig. 11a. A clear trend is visible in the chart, where the cancellation of the non-minimum phase behavior clearly leads to better tracking precision due to a faster transient response. While very negative values of $\overline{x}_{ref}$ lead to a deterioration of tracking performance, the best tracking precision is obtained for $0.2 < \overline{x}_{ref} < 1$, as expected in light of the results obtained in the previous Section 3.2.

The same conclusions can be drawn by observing the trend in the agility quickness performance metric, reported in Fig. 11b. This parameter, calculated as the ratio between the peak load factor and the maximum excursion of the flight path angle, has been previously proposed as a measure of short-term agility for rotorcraft maneuvering in forward flight [36]. In the opinion of the authors, it is also well suited for interpreting the dynamic performance of aircraft capable of DLC. The highest agility quickness is achieved for $\overline{x}_{ref} = 0.8$, in line with results from all previous analyses.

3.4. Altitude hold in turbulent atmosphere

In the present application, the aircraft is required to hold its initial altitude while flying in a turbulent air field. The von Karman turbulence model has been implemented, and a moderate turbulence intensity level has been selected for the test case [37]. In the same way as before, the task is performed exclusively by means of the altitude control channel shown in Fig. 3, with no input from the pilot.

Altitude time histories are shown in Fig. 12. In this case, different features of the trajectories can be identified for different values of the prescribed position of the CCoP. As expected in light of previous results, extreme values of $\overline{x}_{ref}$, as well as the classic PI approach, result in lower frequency oscillations of greater amplitude. On the other hand, due to the cancellation of the non-minimum phase behavior, values of $\overline{x}_{ref}$ between 0 and +1.0 result in higher frequency altitude oscillations of smaller amplitude, i.e. an overall faster and sharper response to the external disturbance. These observations are once again confirmed by the RMS deviation w.r.t. the reference initial altitude $h_{ref}(t) = 0$, reported in Fig. 13a. The trend of $\overline{\Delta h}$ as a function of $\overline{x}_{ref}$ is completely analogous to the one seen in the previous application.

Table 2
Guidelines for the interpretation of the overall frequency-weighted RMS acceleration as an indication of the level of comfort on board [39].

Acceleration magnitude $\overline{a}$ (m/s^2)	Comfort level indication
< 0.315	Not uncomfortable
0.315 – 0.63	A little uncomfortable
0.5 – 1	Fairly uncomfortable
0.8 – 1.6	Uncomfortable
1.25 – 2.5	Very uncomfortable
> 2	Extremely uncomfortable

As a final analysis on these simulations, the overall frequency-weighted RMS acceleration $\overline{a}$ perceived by a passenger seated at the aircraft CG location has been estimated. The methodology described in [38] has been implemented, with reference to the ISO 2631-1 standard [39]. Results are reported in Fig. 13b as a function of the prescribed position of the CCoP. While it is hard to compare the absolute numeric values to similar studies on conventional aircraft of similar category and in similar flight scenarios, the chart once again highlights a trend analogous to all previous cases. The ISO 2631-1 standard also provides guidelines to interpret the numerical values of $\overline{a}$ as a quantitative measure of comfort on board. These are graphically represented on the left side of Fig. 13b and additionally reported in Table 2. As it can be seen, the overall acceleration obtained with the standard PI approach is classified as either “uncomfortable” or “fairly uncomfortable”. On the other hand, the proposed CA approach is able to obtain a consistent improvement, resulting in a clear classification as “little uncomfortable” in the best case.

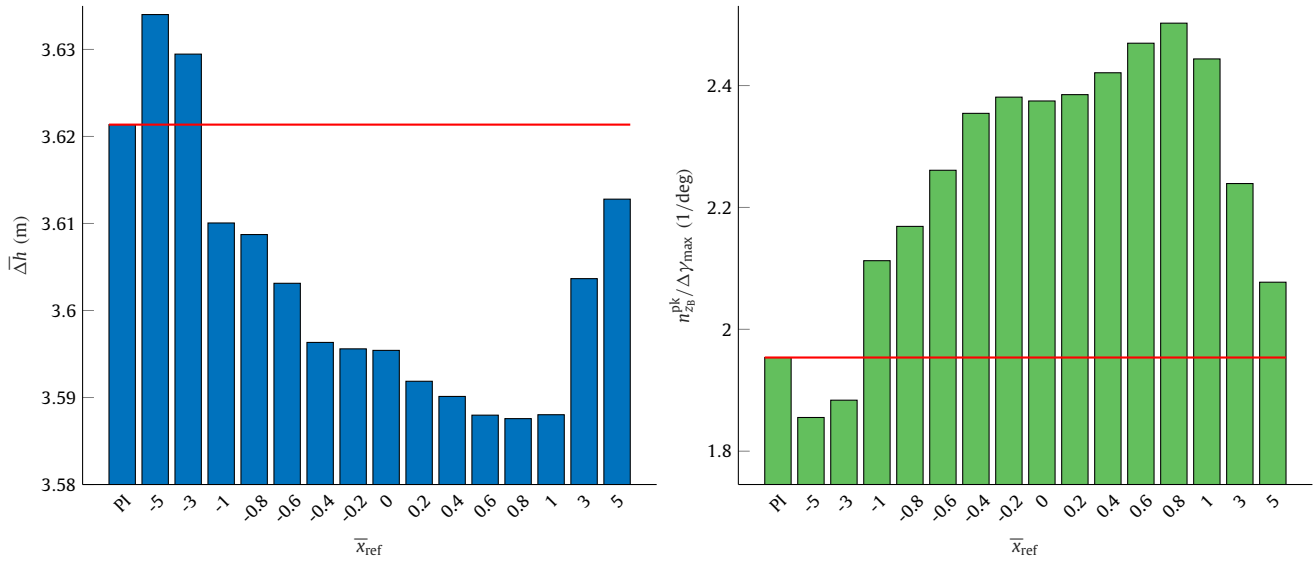

a) Altitude RMS deviation **b)** Agility quickness in the first climb time span ($t < 30$ s)

Fig. 11. Derived performance metrics for the altitude shift task, for different values of the reference CCoP location and the standard PI approach.

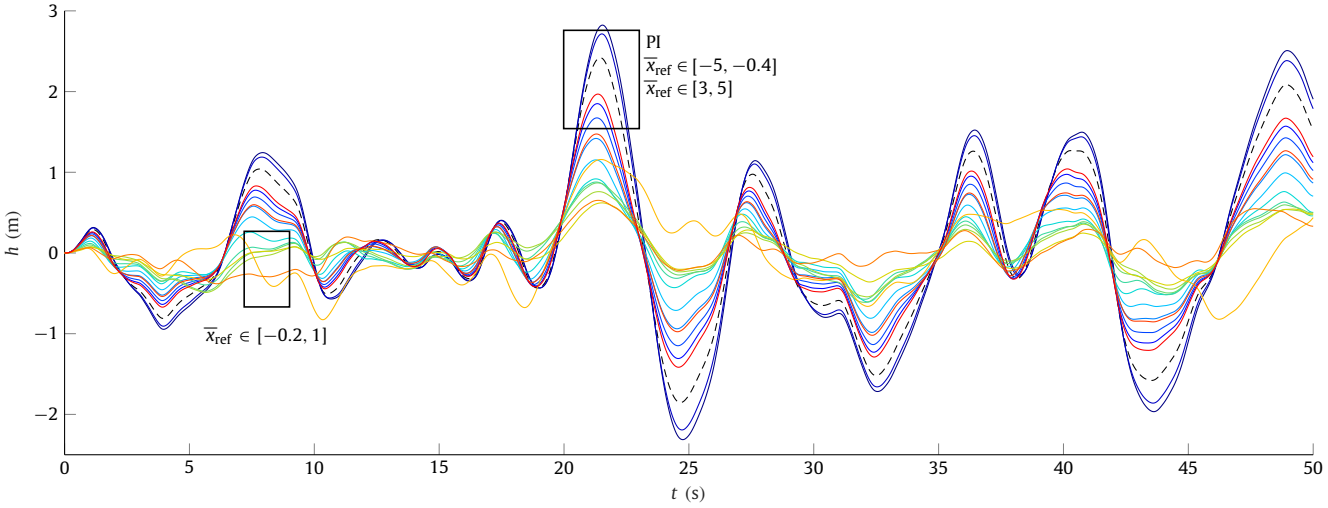

Fig. 12. Altitude time histories for the altitude hold task in turbulent atmosphere, for different values of the reference CCoP location and the standard PI approach. Legend labels have been aggregated, colors match Fig. 7a.

4. Conclusions

A novel Control Allocation (CA) approach has been proposed with the objective of shaping the aircraft transient response by exploiting the concept of Control Center of Pressure (CCoP), i.e. the center of pressure due to only aerodynamic control forces. First, a formulation based on the straightforward augmentation of the control effectiveness matrix has been presented. This can be used to modify any classic CA method already existing, but may result in an ill-conditioned effectiveness matrix in some limit cases. Another formulation, based on a weighting matrix to prioritize effectors, has been outlined and implemented in three applications featuring a box-wing aircraft configuration: a simple pull-up maneuver, a trajectory tracking task, and an altitude holding task in turbulent atmosphere.

The performance of the proposed CA formulation is studied as a function of the prescribed position of the CCoP, and compared to a classic Pseudo Inverse (PI) CA method. Results show that, with the same closed-loop characteristics, the proposed approach can significantly impact performance metrics that are closely related to the aircraft transient response, such as delay due to non-minimum phase behavior, tracking precision, and capability of disturbance rejection. In the best case scenario, the aircraft is able to completely cancel the non-minimum phase behavior typical of pitch dynamics, hence achieving a sharp and more agile initial response to longitudinal commands. This results in improved tracking precision, better disturbance rejection, and ultimately in an improved feeling of comfort on board.

Although the presented CA method is applicable to any aircraft configuration, the obtained results reflect, to some extent, the flight mechanics potential of the box-wing geometry. Thanks to the presence of redundant control surfaces, both fore and aft of the aircraft center of gravity, this configuration allows a large excursion of the CCoP, which is probably infeasible for more conventional architectures. Further research could be therefore devoted to assessing the benefits of the proposed CA approach on conventional aircraft configurations. From a more fundamental standpoint, improving the control effectiveness matrix conditioning problem could make

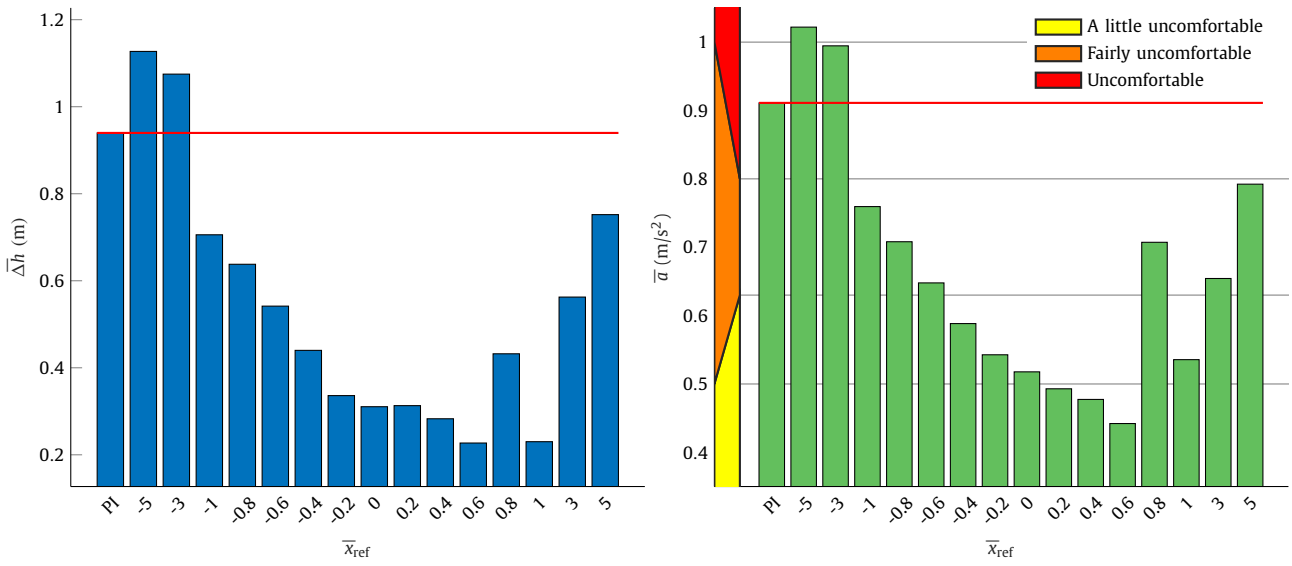

a) Altitude RMS deviation

b) Overall frequency weighted RMS acceleration perceived at the aircraft CG [39]

Fig. 13. Derived performance metrics for the altitude hold task, for different values of the reference CCoP location and the standard PI approach.

the proposed formulation applicable to a wider range of already available CA methods. Lastly, the development of specific flying qualities metrics for DLC longitudinal response remains an open challenge.

Funding

The research presented in this paper has been carried out in the framework of the PARSIFAL (Prandtlplane ARchitecture for the Sustainable Improvement of Future AirpLanes) research project, which has been funded by the European Union within the Horizon 2020 Research and Innovation Program (Grant Agreement No. 723149).

Declaration of competing interest

The authors declare that they have no known competing financial interests or personal relationships that could have appeared to influence the work reported in this paper.

References

[1] R.H. Liebeck, Design of the blended wing body subsonic transport, J. Aircr. 41 (2004) 10–25, https://doi.org/10.2514/1.9084.

[2] B.R. Pascual, R. Vos, The effect of engine location on the aerodynamic efficiency of a flying-v aircraft, in: AIAA Scitech 2020 Forum, American Institute of Aeronautics and Astronautics, 2020.

[3] L. Prandtl, Induced Drag of Multiplanes, NACA Technical Note 182 National Advisory Committee for Aeronautics, 1924, http://naca.central.cranfield.ac.uk/reports/1924/naca-tn-182.pdf.

[4] L. Demasi, G. Monegato, R. Cavallaro, Minimum induced drag theorems for multi-wing systems, in: 57th AIAA/ASCE/AHS/ASC Structures, Structural Dynamics, and Materials Conference, American Institute of Aeronautics and Astronautics, 2016.

[5] A. Frediani, V. Cipolla, E. Rizzo, The PrandtlPlane configuration: overview on possible applications to civil aviation, in: Springer Optimization and Its Applications, Springer US, 2012, pp. 179–210.

[6] K. Abu Salem, V. Cipolla, M. Carini, M. Meheut, S. Kanellopoulos, V. Binante, M. Maganzi, Aerodynamic design and preliminary optimization of a commercial prandtlplane aircraft, https://doi.org/10.13009/EUCASS2019-741, 2019.

[7] T. Stokkermans, L. Veldhuis, B. Soemarwoto, R. Fukari, P. Eglin, Breakdown of aerodynamic interactions for the lateral rotors on a compound helicopter, Aerosp. Sci. Technol. 101 (2020) 105845, https://doi.org/10.1016/j.ast.2020.105845.

[8] S. de Wringer, C. Varriale, F. Oliviero, A generalized approach to operational, globally optimal aircraft mission performance evaluation, with application to direct lift control, Aerospace 7 (2020) 134, https://doi.org/10.3390/aerospace7090134.

[9] M. Voskuijl, J. de Klerk, D. van Ginneken, Flight mechanics modeling of the PrandtlPlane for conceptual and preliminary design, in: Springer Optimization and Its Applications, Springer US, 2012, pp. 435–462.

[10] C. Varriale, M. Voskuijl, L.L. Veldhuis, Trim for maximum control authority using the attainable moment set, in: AIAA Scitech 2020 Forum, American Institute of Aeronautics and Astronautics, 2020.

[11] W.J.G. Pinsker, The Control Characteristics of Aircraft Employing Direct-Lift Control, Reports and Memoranda 3629, Royal Aircraft Establishment Aerodynamics Department, 1968, http://naca.central.cranfield.ac.uk/reports/arc/rm/3629.pdf.

[12] R. Merat, Study of a direct lift control system based on the a380 aircraft, in: 46th AIAA Aerospace Sciences Meeting and Exhibit, American Institute of Aeronautics and Astronautics, 2008.

[13] T. Lombaerts, G. Looye, Design and flight testing of nonlinear autoflight control laws incorporating direct lift control, in: Advances in Aerospace Guidance, Navigation and Control, Springer, Berlin Heidelberg, 2013, pp. 549–568.

[14] W.E. McNeill, R.M. Gerdes, R.C. Innis, J.D. Ratcliff, A Flight Study of the Use of Direct-Lift-Control Flaps to Improve Station Keeping During in-Flight Refueling, Technical Memorandum X-2936 NASA, 1973, https://core.ac.uk/download/pdf/80638445.pdf.

[15] A. Tomczyk, Aircraft maneuverability improvement by direct lift control system application, Aerosp. Sci. Technol. 9 (2005) 692–700, https://doi.org/10.1016/j.ast.2005.09.004.

[16] T.A. Johansen, T.I. Fossen, Control allocation—a survey, Automatica 49 (2013) 1087–1103, https://doi.org/10.1016/j.automatica.2013.01.035.

[17] M. Bodson, Evaluation of optimization methods for control allocation, J. Guid. Control Dyn. 25 (2002) 703–711, https://doi.org/10.2514/2.4937.

[18] S.M. Waters, M. Voskuijl, L.L. Veldhuis, F.J. Geuskens, Control allocation performance for blended wing body aircraft and its impact on control surface design, Aerosp. Sci. Technol. 29 (2013) 18–27, https://doi.org/10.1016/j.ast.2013.01.004.

[19] C. Huijts, M. Voskuijl, The impact of control allocation on trim drag of blended wing body aircraft, Aerosp. Sci. Technol. 46 (2015) 72–81, https://doi.org/10.1016/j.ast.2015.07.001.

[20] F.A. de Almeida, Robust off-line control allocation, Aerosp. Sci. Technol. 52 (2016) 1–9, https://doi.org/10.1016/j.ast.2016.02.002.

[21] X. Lang, A. de Ruiter, A control allocation scheme for spacecraft attitude stabilization based on distributed average consensus, Aerosp. Sci. Technol. 106 (2020) 106173, https://doi.org/10.1016/j.ast.2020.106173.

[22] W.C. Durham, J.G. Bolling, K.A. Bordignon, Minimum drag control allocation, J. Guid. Control Dyn. 20 (1997) 190–193, https://doi.org/10.2514/2.4018.

[23] M. Oppenheimer, D. Doman, A method for including control effector interactions in the control allocation problem, in: AIAA Guidance, Navigation and Control Conference and Exhibit, American Institute of Aeronautics and Astronautics, 2007.

[24] S.A. Frost, M. Bodson, J.J. Burken, C.V. Jutte, B.R. Taylor, K.V. Trinh, Flight control with optimal control allocation incorporating structural load feedback, J. Aerosp. Inform. Syst. 12 (2015) 825–834, https://doi.org/10.2514/1.i010278.
[25] J. Liu, W. Zhang, X. Liu, Q. He, Y. Qin, Gust response stabilization for rigid aircraft with multi-control-effectors based on a novel integrated control scheme, Aerosp. Sci. Technol. 79 (2018) 625–635, https://doi.org/10.1016/j.ast.2018.06.022.
[26] J.K. Nathman, VSAERO 7.9: A Computer Program for Calculating the Nonlinear Aerodynamic Characteristics of Arbitrary Configurations, Stark Aerospace, Inc, 8440 154th Avenue NE, Redmond, Washington, DC, USA, 2016.
[27] P.-J. Proesmans, Preliminary Propulsion System Design and Integration for a Box-Wing Aircraft Configuration, mathesis, Delft University of Technology, 2019, http://resolver.tudelft.nl/uuid:0d2ebc46-09ee-493f-bb4c-c871133bff6f.
[28] C. Varriale, K. Hameeteman, M. Voskuijl, L.L. Veldhuis, A thrust-elevator interaction criterion for aircraft optimal longitudinal control, in: AIAA Aviation 2019 Forum, American Institute of Aeronautics and Astronautics, 2019.
[29] C. Varriale, A. Raju Kulkarni, G. La Rocca, M. Voskuijl, A hybrid, configuration-agnostic approach to aircraft control surface sizing, in: 25th International Congress of the Italian Association of Aeronautics and Astronautics (AIDAA), 2019.
[30] D. van Ginneken, M. Voskuijl, M. van Tooren, A. Frediani, Automated control surface design and sizing for the Prandtl plane, in: 51st AIAA/ASME/ASCE/AHS/ASC Structures, Structural Dynamics, and Materials Conference, American Institute of Aeronautics and Astronautics, 2010.
[31] A.R. Kulkarni, C. Varriale, M. Voskuijl, G.L. Rocca, L.L. Veldhuis, Assessment of sub-scale designs for scaled flight testing, in: AIAA Aviation 2019 Forum, American Institute of Aeronautics and Astronautics, 2019.
[32] G.J.J. Ducard, Fault-Tolerant Flight Control and Guidance Systems, Springer-Verlag GmbH, 2009, https://www.ebook.de/de/product/12471973/guillaume_j_j_ducard_fault_tolerant_flight_control_and_guidance_systems.html.
[33] W. Durham, K.A. Bordignon, R. Beck, Aircraft Control Allocation, Wiley, 2017, https://www.ebook.de/de/product/26657045/wayne_durham_kenneth_a_bordignon_roger_beck_aircraft_control_allocation.html.
[34] S. Kim, K.R. Horspool, Nonlinear controller design for non-minimum phase flight system enhanced by adaptive elevator algorithm, https://doi.org/10.2514/6.2020-0603, 2020.
[35] US Department of Defense, Flying Qualities of Piloted Aircraft, MIL-STD-1797A Handbook, 1997.
[36] M.D. Pavel, G.D. Padfleld, The extension of ADS-33—metrics for agility enhancement and structural load alleviation, J. Am. Helicopter Soc. 51 (2006) 319, https://doi.org/10.4050/jahs.51.319.
[37] T. von Karman, L. Howarth, On the statistical theory of isotropic turbulence, Proc. R. Soc. Lond. Ser. A, Math. Phys. Sci. 164 (1938) 192–215, https://doi.org/10.1098/rspa.1938.0013.
[38] E.F. Trollip, J.A.A. Engelbrecht, Ride comfort in commercial aircraft during formation flight using conventional flight control, in: 2016 IEEE Aerospace Conference, IEEE, 2016.
[39] ISO 2631-1, Mechanical Vibration and Shock — Evaluation of Human Exposure to Whole-Body Vibration, International Organization for Standardization, 1997, https://www.iso.org/standard/7612.html.